LEBEDEV PHYSICAL INSTITUTE
RUSSIAN ACADEMY OF SCIENCES


PREPRINT

9

B. A. BRYUNETKIN, V. S. BELYAEV,
A. P. MATAFONOV, N. N. DEMCHENKO,
V. B. ROZANOV, G. A. VERGUNOVA,
E. M. IVANOV

# THE RADIATIVE LOSSES OF THE PLASMA AT INTERACTION OF ULTRA-SHORT LASER PULSES WITH MATTER.

Moscow 2001

# THE RADIATIVE LOSSES OF THE PLASMA AT INTERACTION OF ULTRA-SHORT LASER PULSES WITH MATTER.

[1]B. A. BRYUNETKIN, [2]V. S. BELYAEV, [2]A. P. MATAFONOV,
[3]N. N. DEMCHENKO, [3]V. B. ROZANOV, [3]G. A. VERGUNOVA, [4]E. M. IVANOV

[1]*State Scientific Center «All Russian Research Institute of Physical-Technical and Radio-Technical Measurements» (VNIIFTRI), Mendeleevo*
[2] *Central research institute of machine building (TSNIIMASH), Korolev*
[3]*P.N. Lebedev Physical Institute of RAS (FIAN), Moscow*
[4]*Moscow State Engineering Physics Institute (Technical University) (MIFI)*

## ABSTRACT

The radiative losses of the plasma produced by ultra-short laser pulses at the surface of solid targets were investigated by means of the methods of high-resolution X-ray spectroscopy and with the help of numerical simulation of hydrodynamic and radiative processes. The experiments were carried out on a laser facility "Neodim" at TSNIIMASH. The surface of Al and Cu solid targets was irradiated by laser pulses of $10^{17}$ W/cm$^2$ radiation density. The temporally integrated linear spectra of the multi-charged ion plasma were recorded to be of 0.8 to 3.0 keV, in soft X-ray. The comparison of experimental spectrums with numerical calculations results on models, including hydrodynamical and radiative-collisional processes, was carried out. The observed relation between a dynamics of radiation of separate groups of lines with a spatial and temporal dynamics of a laser flare permits one to speculate about the nonstationary processes that proceed in the plasma even by analyzing the time-unresolved spectra. From a comparison of experimental and calculations results it follows that a linear radiation of a small group of ions constitutes the main part of radiative losses.

*e-mail* **ievgeny@beep.ru** or **opacity@yandex.ru**

## §1. Introduction, formulation of the problem.

The aim of the work is the interpretation of experimental results obtained at TSNIIMASH on the "Neodim" laser facility in the course of laser interaction experiments performed with solid targets irradiated by picosecond laser pulses at the radiation flux density $\boldsymbol{I} \geq 10^{17}$ W/cm$^2$. The experimental and theoretical studies of an interaction of super-power ultra-short laser pulses with matter are currently an active area of investigation. In this work, we employ both the methods of high-resolution X-ray spectroscopy and the results of numerical simulation of hydrodynamic and radiative processes for studying the radiative losses of the plasma produced by such pulses at the surface of solid targets.

As seen from the experimental and theoretical results that follow, a behavior of the laser pulse interaction with a target essentially depends on the presence of prepulse that precedes the main pulse. Even a small-energy prepulse (~$3\cdot10^{-4}$ of the main pulse radiation density, in our case) may create a plasma that expands in space during a time delay between a prepulse and a main pulse which is considerably longer than their duration. As a result, the main pulse would interact not with a solid matter, but with quite a rarefied and lengthy plasma.

## §2. Experimental setup.

The experiments were carried out at TSNIIMASH (town of Korolev) on a laser facility "Neodim" (laser energy up to 1.5 J in 1 ps pulse at the fundamental wavelength of 1.055 μm) [1]. The surface of Al and Cu solid targets was irradiated by laser pulses of $10^{17}$ W/cm$^2$ radiation density. The temporally integrated linear spectra of the multi-charged ion plasma were recorded to be of 0.8 to 3.0 keV, in soft X-ray, by means of a Bragg spectrograph with plane (CsAP) and spherically bent (mica) crystals [2]. A diagnostics of time-averaged temperature and density of free electrons in the plasma, near a target surface, was carried out on the basis of experimentally measured line intensities using the models of a level kinetics.

Figure 1 illustrates a scheme of a 5 TW laser facility "Neodim" that consists of the following subsystems:

1 – master oscillator with a passive mode locking and negative feedback having an active element of neodymium phosphate glass GLS-22 sized ∅5 x 100 mm$^2$;
2 – a stretcher consisting of two holographic diffraction gratings and a telescope between them;
3 – regenerative amplifier with an active element of neodymium phosphate glass GLS-22 sized ∅5 x 100 mm$^2$;
4 – an amplifying system consisting of three amplifiers with active elements of GLS-22 glass sized ∅ 20 x 300 mm$^2$; ∅ 30 x 300 mm$^2$, and ∅ 45 x 300 mm$^2$;
5 – a compressor consisting of two holographic diffractive gratings sized 110 x 180 mm$^2$.

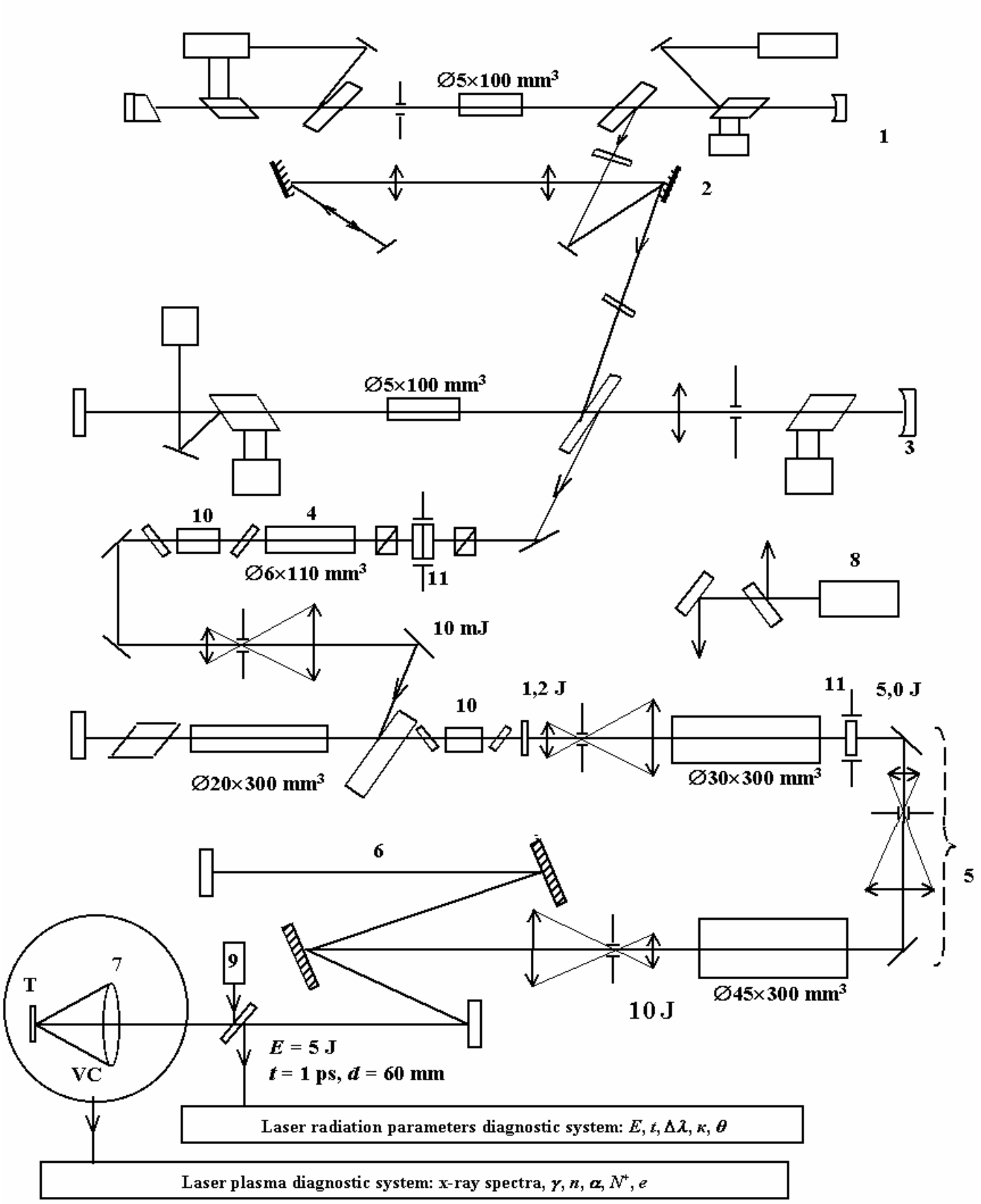


**Fig.1.** Schematic representation of a 5 TW power "Neodim" laser facility.
1 – master oscillator, 2 – stretcher, 3 – regenerative amplifier, 4 – preamplifier of Ø6x110 mm$^3$; 5 – amplifying system consisting of three amplifiers; 6 – compressor, 7 – focusing system; 8,9 – adjustable laser at λ=1.06 μm; 10 – Faraday cell; 11 – Pockells cell shutter; T – target; VC – vacuum chamber

A laser pulse, at the output from a compressor, has energy of 1÷5 J and pulse duration of 1 ps at the radiation divergence close to diffraction. A part of the laser radiation goes to the means of the laser parameter diagnostics, namely: an auto-correlator for laser pulse duration measurements; a spectral monitor for laser pulse spectral registration; a beam aperture monitor of a laser radiation power distribution; a power meter of single pulses. The main of the 1÷5 J laser radiation goes to a focusing system with a 6-cm diameter non-spherical objective, which provides $10^{17}$-$10^{18}$ W/cm$^2$ radiation intensity on a target.

Figure 2 demonstrates the spectrograms of plasma containing multi-charged ions of aluminum and copper obtained at the interaction of picosecond laser pulses with plane massive targets made of these elements. An incidence angle of the laser radiation (***p***-polarization) was ~22$^o$ of a target normal. The spectrographs were mounted about at the same angle. The densitograms of these spectra, an identification of most typical spectral lines, and a comparison of the densitograms with the calculations results are presented in section 4.

a) Al

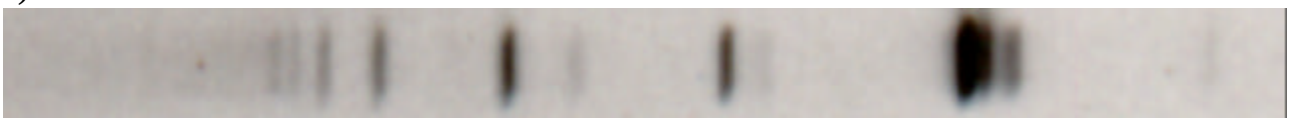

b) Cu

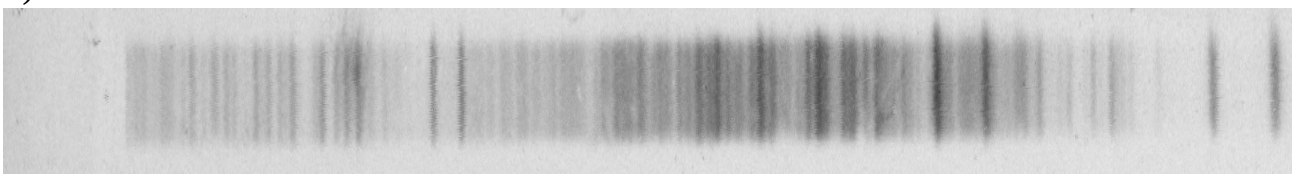

**Fig.2.** Spectrograms of an aluminum (a) and copper (b) plasma radiation obtained at a picosecond laser pulse interaction with a target.

## §3. Calculations of the plasma evolution.

In this section, we present the calculation results of the plasma evolution at the interaction of a picosecond laser pulse with matter with account of a prepulse. The laser plasma processes were considered on the basis of qualitative estimates and a numerical simulation using the RAPID-SP [3] and RADIAN [4] codes.

A physical model of the RAPID-SP code is based on the equations of a single-liquid two-temperature hydrodynamics (a one-dimensional model for a plane symmetry) with account of a ponderomotive force and a Maxwell equation for the laser radiation at tilt incidence in the case of *s*- and *p*- polarizations. It is assumed that the time of light propagation in the plasma is less than a sound wave period. The generation of fast electrons in the plasma resonance at a critical surface is also taken into account in this model, as well as the electron transport, with account of frictional force due to the ionization losses. A physical-mathematical model and the simulation results of a laser interaction with matter are described in more detail in [3]. The following initial data were accepted in the calculations: intensity of the main pulse, $q_0=10^{17}$ W/ñm$^2$, intensity of a prepulse, $3\cdot10^{13}$ W/ñm$^2$. The main pulse and the prepulse had a triangular shape of 1 ps duration FWHM. A delay time of the main pulse was 13 ns.

Figures 3 and 4 illustrate the calculations results of the plasma parameters for two moments, i.e. 13.002 ns, corresponding to a moment immediately after the main pulse cessation and 13.200 ns, in 198 ps after the pulse cessation. Figure 1 depicts the results for an aluminum plasma, and Fig.2, for a copper plasma. The density profiles for both materials proved to be highly modulated at the moment of the pulse cessation. This is due to a formation of a sub-critical region of the plasma under the action of thermal and ponderomotive pressure. A ponderomotive potential of this region turns out to be highly modulated in space due to the interference of the incident and reflected laser radiation waves. The density profiles and the plasma velocity are modulated under the action of a ponderomotive force. One should note high value of an ion temperature that arises as a result of dissipation of the ion pertubations.

The RADIAN code [4] is based on a physical model that includes absorption of an external laser radiation, an equation system that describes a two-temperature gas dynamics, a thermonuclear ignition, and a transfer of ?-particles. The radiation field is determined by a quasi-stationary transfer equation. A two-dimensional evaporation of a plane target was simulated by a 1D calculation of heating and motion of a spherical target with a radius equal to a focal spot diameter (~30 μm). The energy absorption was provided by a Bremsstrahlung process. The initial conditions of the calculations were as follows: a prepulse intensity $10^{12}$ W/ñm$^2$, a main pulse intensity, $10^{16}$ W/ñm$^2$, and a delay time, 13 ns.

Figure 5 demonstrates the calculations results of the temperature and density profiles for the above conditions. A calculation of a laser plasma radiation density q [W/cm$^2$] is plotted in this Figure too.

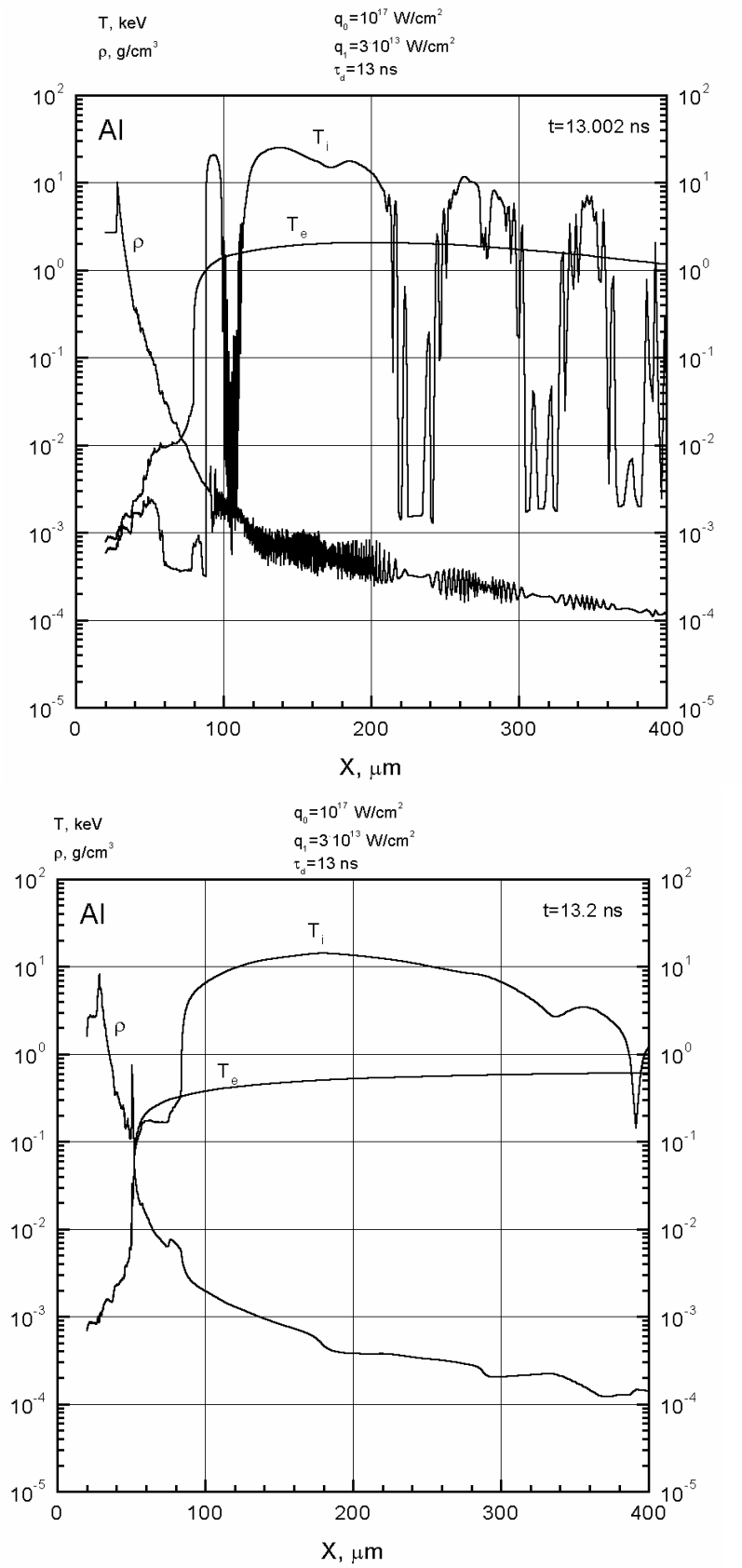


**Fig.3.** Profiles of density, ?, electron $T_e$ and ion $T_i$ temperatures at the moments 13.002 ns (immediately after a cessation of the main pulse, top), and 13.200 ns (in 198 ns after the main pulse, bottom) for an aluminum plasma.

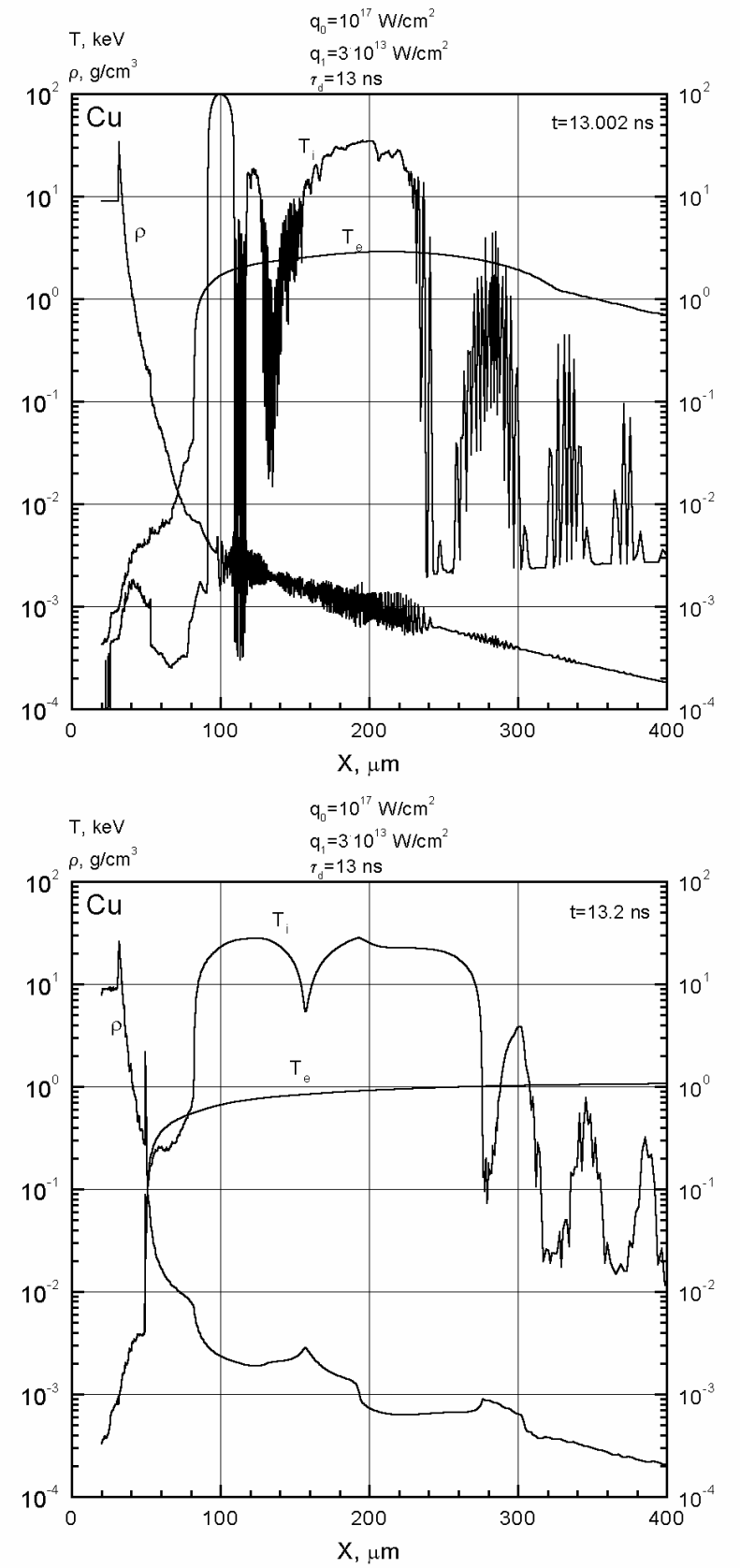


**Fig.4.** Profiles of density ?, electron $T_e$ and ion $T_i$ temperatures at the moments 13.002 ns (immediately after a cessation of the main pulse, top), and 13.200 ns (in 198 ns after the main pulse, bottom) for a copper plasma.

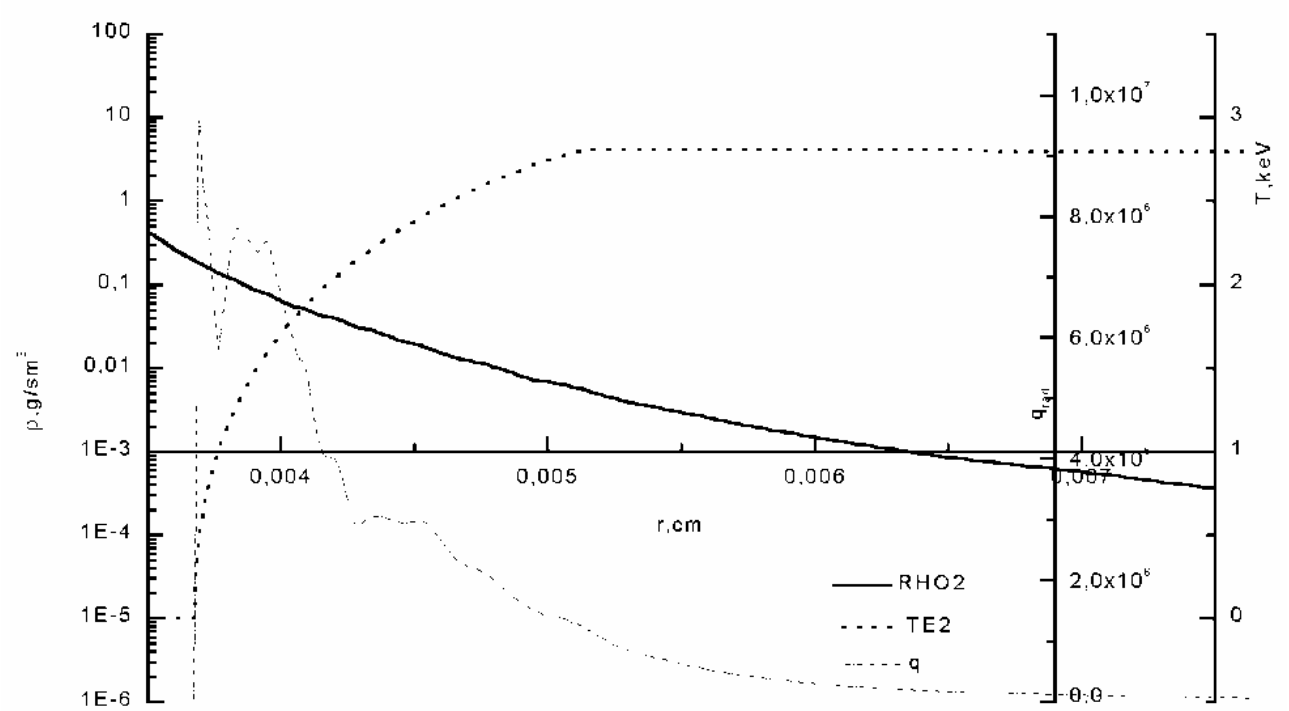


**Fig.5.** Density ? and electron temperature $T_e$ profiles after an action of prepulse on the plasma with $10^{12}$ W/ñm$^2$ intensity and the main pulse with $10^{16}$ W/ñm$^2$ intensity.

## §4. Calculation of optical characteristics of the plasma.

As shown by the calculation results, the temperature and density of the plasma are changing within a wide range under experimental conditions on a "Neodim" laser facility. The plasma can both be under the ionization equilibrium conditions (coronal or local thermodynamic) and in the absence of equilibrium. Thus, in order to describe the plasma processes one can't use sufficiently simple relationships describing ionization state densities and the populations of levels at equilibrium. The optical properties of the plasma were calculated by a collision-radiative model [5], [6] and the computer codes developed on its base. The model takes into account all the basic processes that participate in the ion distribution over the ionization degrees and the excitation levels, namely: the spontaneous radiative transitions, collision excitation and deactivation, electron collision ionization, three-body collision recombination, photo-recombination, and a dielectronic recombination. An optically transparent plasma, having a Maxwell electron velocity distribution, has been considered.

The calculations of spectral and spectrally integrated radiation losses of the plasma were carried out with account of the bremsstrahlung, recombination, and line radiation. A spectral emissivity (density of the radiation power emitted in a single solid angle in a single spectral range) is calculated as:

$$j_\nu = 5\cdot 10^{12}(h\nu)^3_{[keV]}\left\{\sum_Z\sum_m\sum_{n>m} N_n^Z \frac{g_m}{g_n}\sigma_{mn}^{bb}(\nu) + \sum_Z\sum_{n,\,m} N_n^{Z+1}\sigma_{nm}^{fb}(\nu)e^{-h\nu/kT} + \right.$$

$$\left. + \sum_Z N_i N_e \sigma^{ff}(\nu) e^{-h\nu/kT}\right\}, \left[\frac{W}{ñm^3\cdot eV\cdot ster}\right] \qquad (1)$$

where *hn* is the photon energy in keV; $N_n^Z$ , the population of the level *n* of a *Z* ion; $g_m$ and $g_n$, the statistical weights of the lower and upper levels, respectively; $s_{mn}^{bb}(n)$, the cross-section of absorption in a line at transition from *m* level to *n* level; $s_{nm}^{fb}(n)$, photo-recombination cross-section on the *m*-level; $s^{ff}(n)$ determines a cross-section of a bremsstrahlung absorption, and $N_i$ and $N_e$ are the ion and electron concentrations, respectively. We used the Kramers quasi-classical expressions [7] for the cross-sections of free-free and free-bound transitions. The data for the absorption cross-sections in the lines (or the oscillator forces $f_{mn}$ and the transition probabilities that are proportional to them) were borrowed from the experimental and calculation results available in the literature. The absorption cross-section is defined by:

$$\sigma_{mn}^{bb} = \frac{\pi e^2}{m_e \tilde{n}} f_{mn} \Psi(\nu) \qquad (2)$$

where *Y(n)* is the line profile normalized per unit. As the line profile we used the Voigt profile

$$\Psi(\nu) = \frac{\gamma}{2\pi} \frac{1}{\sqrt{\pi} v_0} \int_0^{\infty} \frac{\exp\left(-(v / v_0)^2\right) \cdot dv}{(\nu - \nu_{mn} - \nu_{mn} v/c)^2 + (\gamma/2)^2} \qquad (3)$$

where *g* is the total homogeneous spectral linewidth ($g=g_r+g_{qs.}$).

In the calculations, we took into account natural, Doppler, and collisional broadening of spectral lines. In addition, we used an instrumental broadening, *l/Dl=800*, to obtain an agreement with the experimental spectra. The widths of the spectra lines are defined by:

*a)* a natural width, $?_r$

$$\gamma_r = \frac{2e^2\omega_{mn}^2}{3mc^3} \text{ or } \Delta E_r = 9{,}6\,10^{-6}(h\nu)^2_{[keV]}[keV], \text{where } h\nu = E_n - E_m,\ n > m \qquad (4a),$$

*b)* a Doppler width, $?_D$

$$g_D = 2\sqrt{\ln 2} w_{mn} \frac{v_0}{c},\ v_0 = \sqrt{\frac{2kT}{M}} \text{ or } \Delta E_D = 2{,}4\,10^{-3}(hn)_{[keV]}\sqrt{T_{[kev]}/M}\ [keV] \qquad (4b),$$

where $n_o$ is the most probable ion velocity at Maxwell distribution and *M* is the atomic mass of an element. (Only Doppler broadening, connected with thermal motion of the ions, was taken into account in calculations. However in the experiment the main contribution to the Doppler broadening is connected with motion of the plasma as a whole. The velocity of such motion is comparable with the characteristic thermal velocity of ions).

*c)* a quasi-stationary width, $g_{qs.}$

$$\gamma_{qs.}=6{,}0\ 10^{-10}\ (T_e / M)^{1/2}\ N_i^{1/3}\ [\text{keV}] \qquad (4c)$$

Now consider the calculation results of the emissivities of the plasma. The calculations were made for the aluminum and copper plasmas. In further calculations and analysis one has chosen the (Ò, ?) pairs (Table 1). (Note that because the temporally integrated spectra had been measured, the calculation conditions were chosen both for 13.002 ns and 13.2ns on the basis of the calculated profiles).

**Table 1**. Parameters of the plasma used in the calculations

| Element | Al | | Cu | |
|---|---|---|---|---|
| ? [g/cm$^3$] \ $T_e$ [keV] | 0.50 | 0.70 | 0.55 | 0.60 |
| $10^{-3}$ | v | v | v | v |
| $10^{-2}$ | v | v | v | v |

Figures 6 and 7 illustrate the calculation results of the spectral emissivity for Al and Cu plasma using the parameters of Table 1. For Al, the results are given within the spectral range 5?8 A (Fig.6), and for Cu, within 7.5?13 A (Fig.7).

To obtain a more accurate comparison with the experimental data, Fig.8 illustrates the calculations results of the spectra for Al (?=2.6·$10^{-3}$ g/ñm$^3$ and T=0.5 keV) and for Cu (?=2.6·$10^{-3}$ g/ñm$^3$ and T=0.55 keV). In this case, the chosen density of matter corresponds to a critical value of the electron concentration $N_e=10^{21}$ ñm$^{-3}$ for the radiation wavelength ?=1.06 μm. The aluminum plasma spectra were chosen so that the integral emissivity for the most intensive spectral lines approximately coincided. The transitions of spectral lines that are present in the calculated spectra are identified in Table 3.

Figure 9 illustrates the calculation results for Al and Cu spectra within the total spectral range where the spectral peculiarities are exhibited (lines and recombination edges). From the Figures it is seen that a considerable part of the integral emissivity of the plasma lies within the spectral range of the experimental measurements (1.55?2.48 keV for aluminum and 0.95?1.65 keV for copper) for the given density and temperature of the plasma.

Figure 10 shows the calculation results for an average ionization, power of the radiative losses per unit plasma $P_{rad}$ [W/ñm$^3$], and the power of radiative losses per one ion $W_{rad}$ [W/ion] for the Al and Cu plasma. The results are reported for t=13.2 ns (in 198 ns after a cessation of the main pulse) The results are reported for a region where the spectral-radiative losses are maximal (20?70 μm). From Fig. 10 it is seen that average ionization “depicts” changes in electron temperature, and the maximum power of the radiative losses per one ion is within the range of the highest temperature gradients. In addition, one can observe a distinct correlation between the separate local maxima at the density profile, and the maxima at the radiative losses per unit plasma volume.

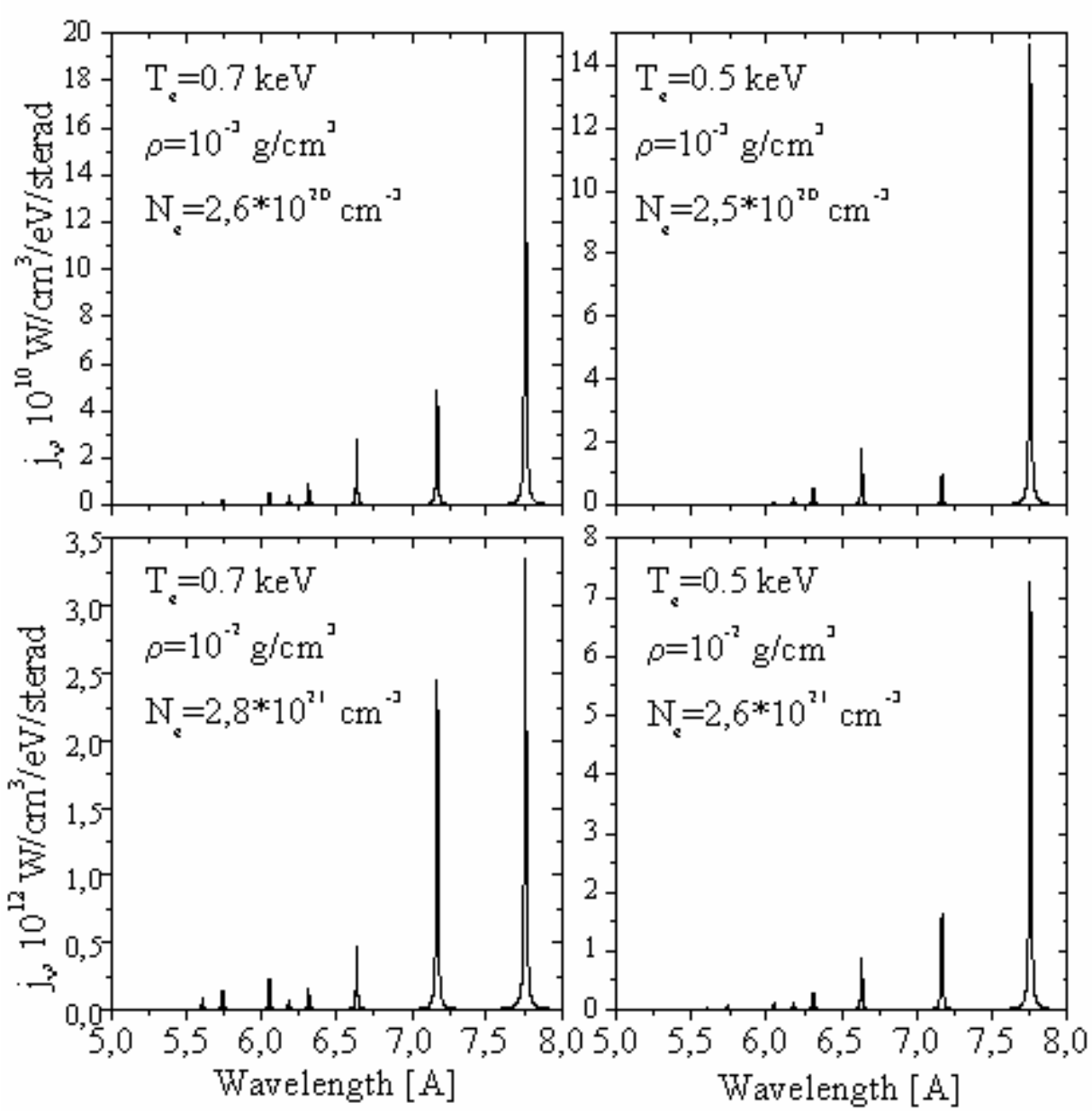


**Fig.6.** Spectral emissivity of Al plasma at different conditions.

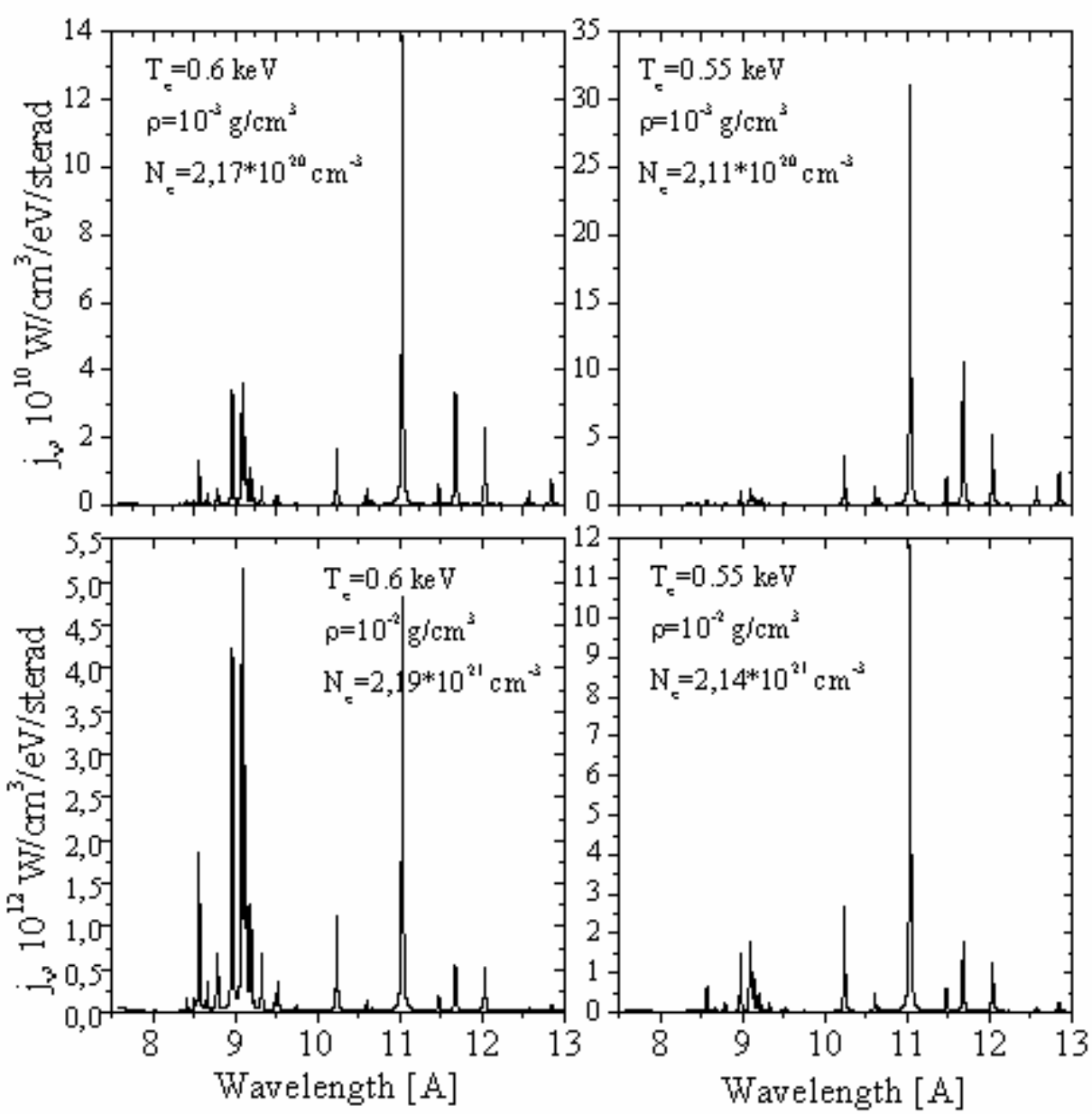


.

**Fig.7.** Spectral emissivity of Cu plasma at different conditions.

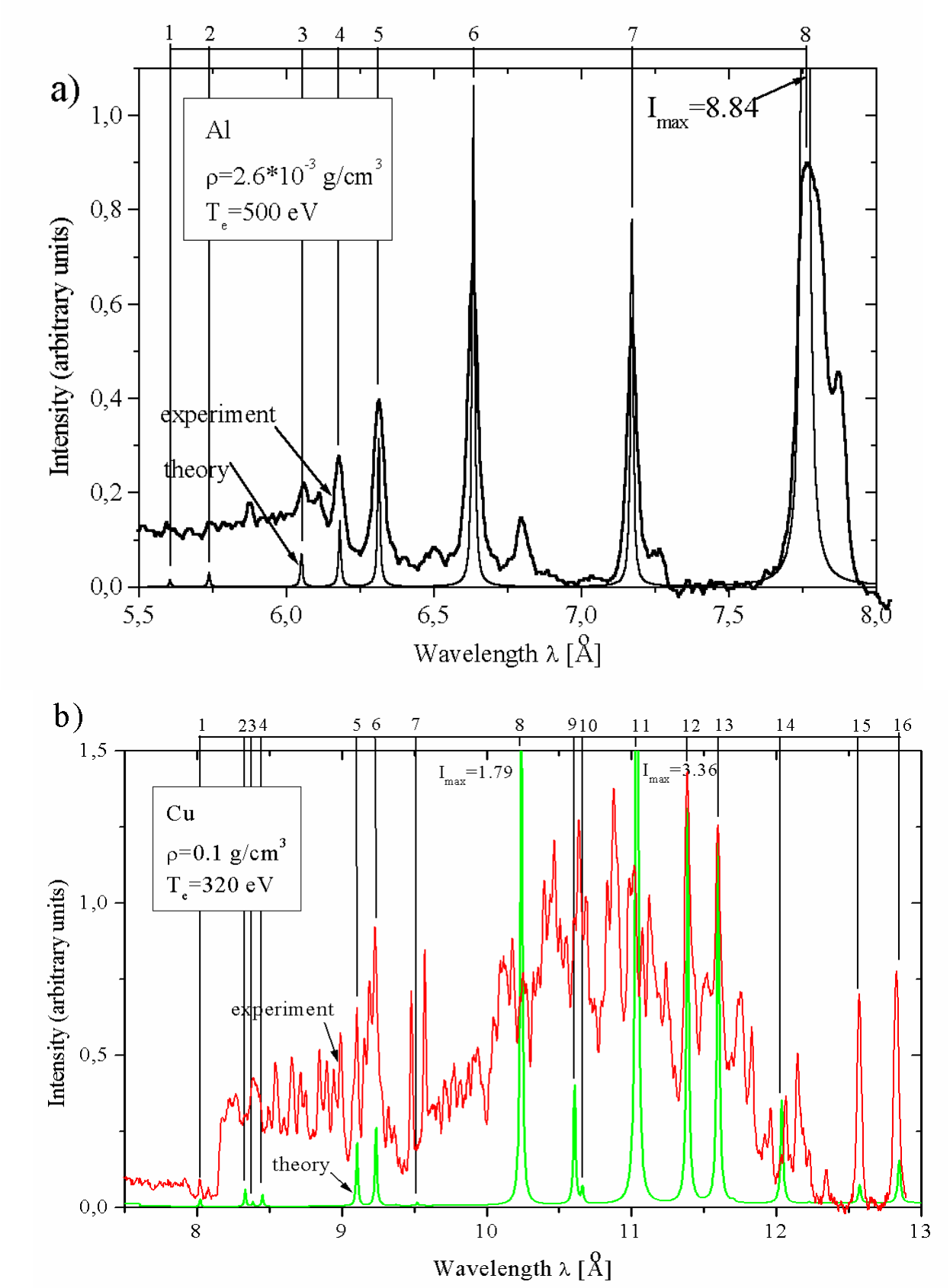


**Fig.8.** Calculated and experimental spectra for the plasma of Al (a) and Cu (b).

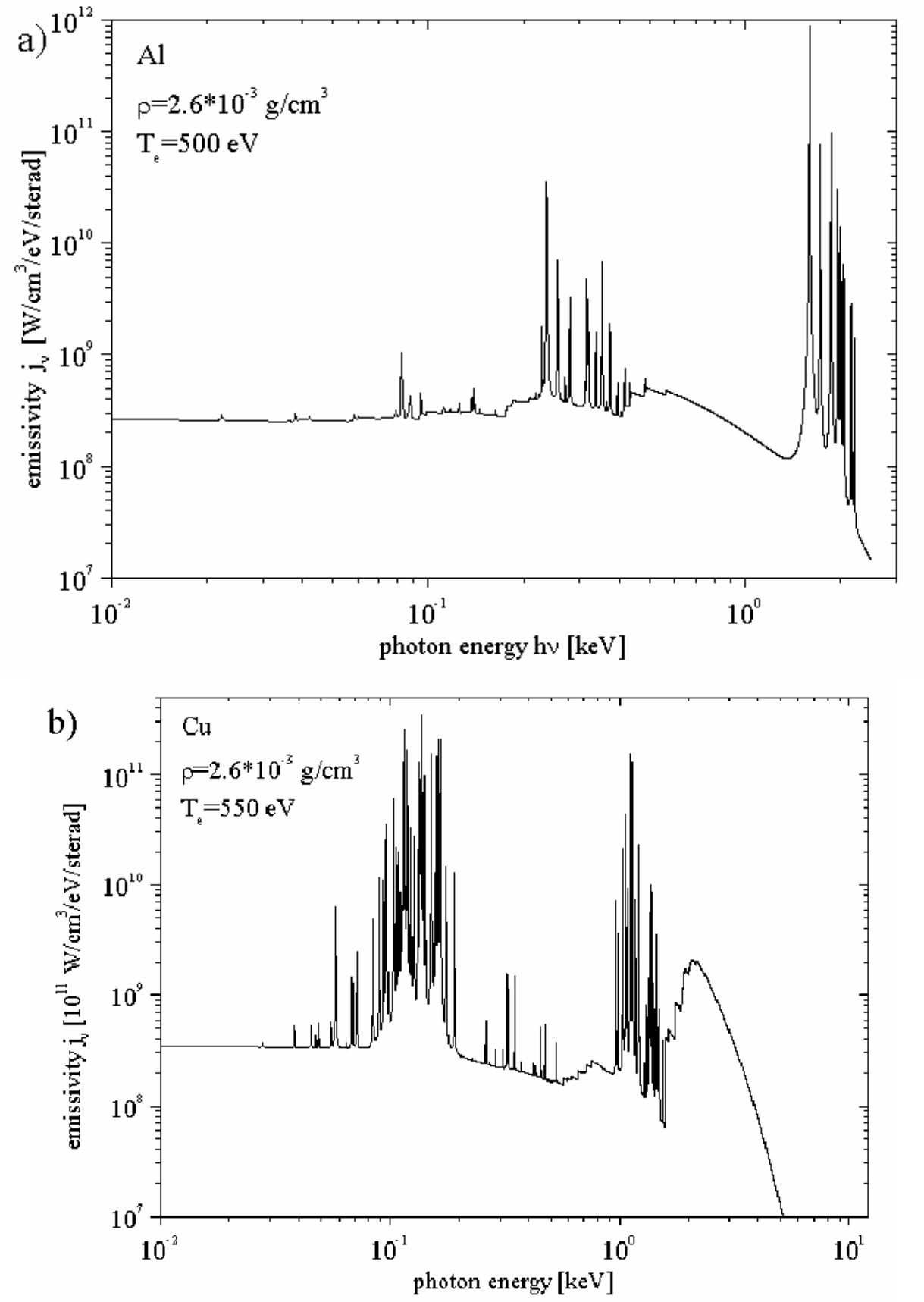


**Fig. 9.** Spectral emissivity for the plasma of Al (a) and Cu (b).

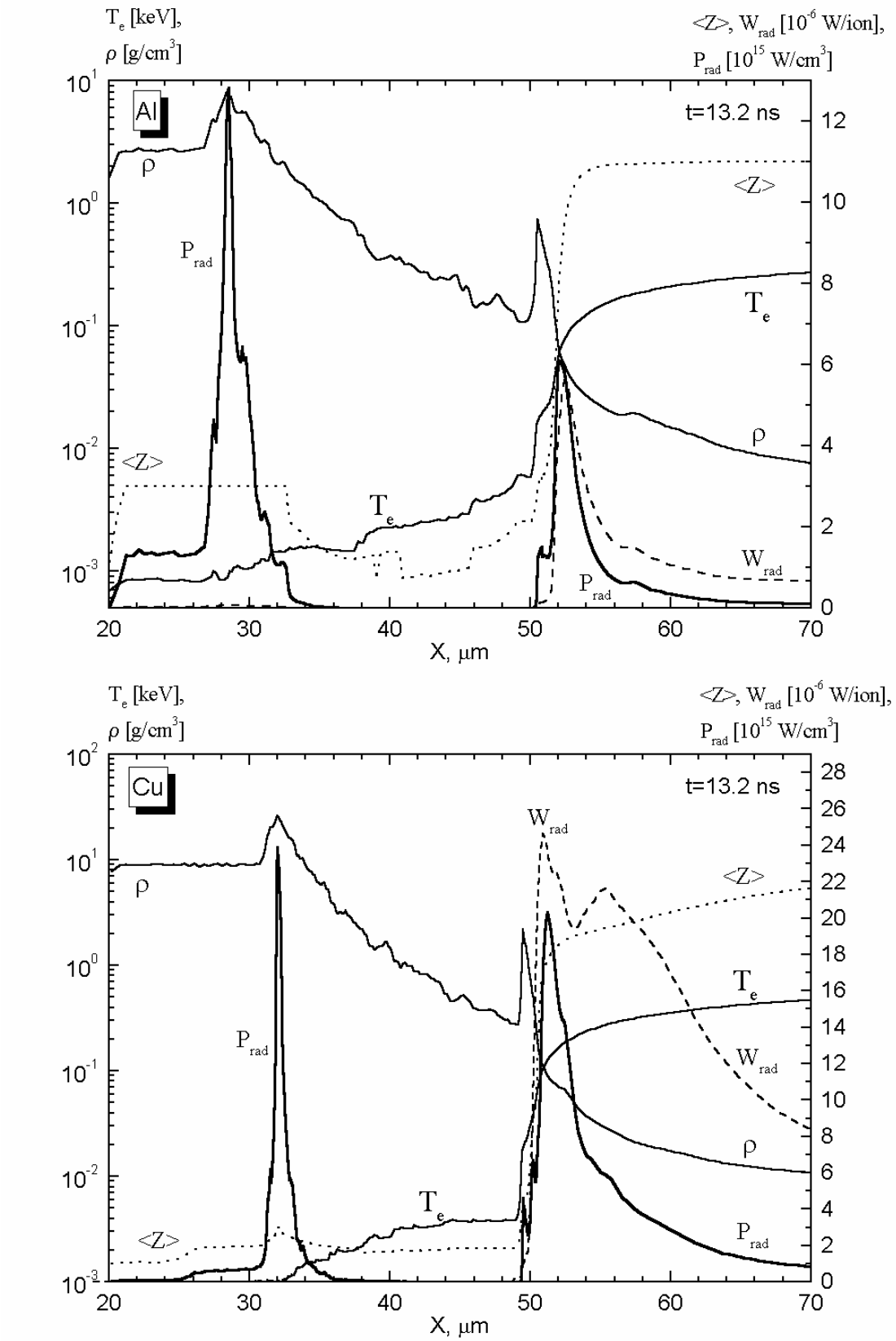


**Fig.10.** The profiles of electron temperature $T_e$, density ρ, average ionization <Z>, power of radiative losses per unit plasma volume $P_{rad}$, and power of radiative losses calculated per one ion $W_{rad}$ for the plasma of Al (top) and Cu (bottom) at 13.2 ns.

## §5. Analysis and interpretation of the results.

In this section, we shall discuss the theoretical and experimental results obtained and present some of the numerical estimates obtained on the basis of these results.
All the data reported were obtained for the experiments on the "Neodim" laser facility under standard Al or Cu target irradiation conditions using the main pulse of 1 J energy at 1 ps duration at ~$10^{17}$ W/ñm$^2$ intensity. At t=-13 ns, a picosecond prepulse of $3\cdot10^{-4}$ J is available ($I_p$~$3\cdot10^{13}$ W/cm$^2$).

To estimate the time of plasma illumination one performed the calculations of the plasma evolution during ~ 200 ps after the main pulse cessation, using the RAPID-SP program. The plasma parameters for 13.002 ns (immediately after the main pulse cessation) and 13.200 ns (in 198 ps after the pulse cessation) are illustrated in Figs. 3 and 4. As seen from these data, the critical density plasma remains hot (T>300 eV) during 200 ps and longer (possibly, ~ 0.5 ns). Such a long X-ray pulse is induced by a laser prepulse which sustains an extended plasma. Dimension of a radiating region may achieve 20?40 μm. The data on the integrated emissivity of Al and Cu plasma, for the conditions of Table 1, are listed in Table 2 (in $10^{13}$ W/ñm$^3$).

**Table 2.** Spectrally integrated emissivity of the plasma.

| Element | Al | | Cu | |
|---|---|---|---|---|
| ? [g/cm$^3$] \ $T_e$ [keV] | 0.50 | 0.70 | 0.55 | 0.60 |
| $10^{-3}$ | 1.02 | 1.68 | 1.10 | 1.07 |
| $10^{-2}$ | 77.1 | 70.5 | 69.1 | 75.7 |

The radiative spectrum for a copper plasma has rather a complex form. We shall consider, therefore, a simpler spectrum of an aluminum plasma (Fig.8a). The main spectral lines are identified in Table 3.

**Table 3**. Characteristics of transitions for most intense spectral lines of the calculation spectra shown in Fig.8.

| No | Ion | Upper level | Lower level | Wavelength [A] (theoretical) | Line spectroscopic designation |
|---|---|---|---|---|---|
| 1 | Al XIII | 5p $^2$P | 1s $^2$S | 5.60 | |
| 2 | Al XIII | 4p $^2$P | 1s $^2$S | 5.74 | |
| 3 | Al XIII | 3p $^2$P | 1s $^2$S | 6.05 | |
| 4 | Al XII | 1s5p $^1$P | 1s$^2$ $^1$S | 6.18 | |
| 5 | Al XII | 1s4p $^1$P | 1s$^2$ $^1$S | 6.31 | |
| 6 | Al XII | 1s3p $^1$P | 1s$^2$ $^1$S | 6.63 | |
| 7 | Al XIII | 2p $^2$P | 1s $^2$S | 7.17 | |
| 8 | Al XII | 1s2p $^1$P | 1s$^2$ $^1$S | 7.76 | |
| | | | | | |
| 1 | Cu XX | 2s$^2$2p$^5$6d $^3$D, $^1$P | 2s$^2$2p$^6$ $^1$S | 8.02 | 6C, 6D |
| 2 | Cu XX | 2s$^2$2p$^5$5d $^1$P | 2s$^2$2p$^6$ $^1$S | 8.33 | 5C |
| 3 | Cu XX | 2s2p$^6$4p $^3$P, $^1$P | 2s$^2$2p$^6$ $^1$S | 8.38 | 4A, 4B |
| 4 | Cu XX | 2s$^2$2p$^5$5d $^3$D | 2s$^2$2p$^6$ $^1$S | 8.45 | 5D |
| 5 | Cu XX | 2s$^2$2p$^5$4d $^1$P | 2s$^2$2p$^6$ $^1$S | 9.10 | 4C |
| 6 | Cu XX | 2s$^2$2p$^5$4d $^3$D | 2s$^2$2p$^6$ $^1$S | 9.23 | 4D |
| 7 | Cu XX | 2s$^2$2p$^5$4s $^3$P | 2s$^2$2p$^6$ $^1$S | 9.52 | 4F, 4G |

| | | | | | |
|---|---|---|---|---|---|
| 8 | Cu XXI | $2s2p^5 3p$ | $2s^2 2p^5\ ^2P$ | 10.23 | |
| 9 | Cu XX | $2s2p^6 3p\ ^1P$ | $2s^2 2p^6\ ^1S$ | 10.60 | 3A |
| 10 | Cu XX | $2s2p^6 3p\ ^3P$ | $2s^2 2p^6\ ^1S$ | 10.66 | 3B |
| 11 | Cu XXI | $2s^2 2p^4 3d$ | $2s^2 2p^5\ ^2P$ | 11.03 | |
| 12 | Cu XX | $2s^2 2p^5 3d\ ^1P$ | $2s^2 2p^6\ ^1S$ | 11.38 | 3C |
| 13 | Cu XX | $2s^2 2p^5 3d\ ^3D$ | $2s^2 2p^6\ ^1S$ | 11.59 | 3D |
| 14 | Cu XXI | $2s^2 2p^4 3s$ | $2s^2 2p^5\ ^2P$ | 12.03 | |
| 15 | Cu XX | $2s^2 2p^5 3s\ ^1P$ | $2s^2 2p^6\ ^1S$ | 12.57 | 3F |
| 16 | Cu XX | $2s^2 2p^5 3s\ ^3P$ | $2s^2 2p^6\ ^1S$ | 12.85 | 3G |

The calculations show that the main contribution of radiation in the basic lines within 5?8 A constitutes ~85% of the radiation in the total range (0?3 keV). To estimate the total energy irradiated by the plasma we shall assume that a volume of a radiating region is equal to the squared size of a focal spot multiplied by the radiative bandwidth $(3\cdot10^{-3}$ ñm$)^2\cdot3\cdot10^{-3}$ ñm ? $3\cdot10^{-8}$ ñm$^3$. Pulse duration of an X-ray emission is 0.5 ns. By assuming that average density of the radiation is ? $2.6\cdot10^{-3}$ g/ñm$^3$, we get a total radiative power of $10^{14}$ W/ñm$^3\cdot3\cdot10^{-8}$ ñm$^3\cdot5\cdot10^{-10}$ s ? $1.5\cdot10^{-3}$ J. As a prepulse at a later stage of a process is ~ 0.5 ns, the density achieves $10^{-2}$ g/ñm$^3$ at rather high temperature (>0.2 keV) the energy of the radiation may be higher and may achieve ?$1.5\cdot10^{-2}$ J. The absorbed and transformed into heat energy of the main pulse will be of 5?10 %. The radiative energy is estimated to be as high as 5% to 50% or higher of the value of an absorbed energy (due to a longer duration of the radiation or higher density in the radiation region). This seems to be reasonable from the physical viewpoint, and does not contradict the experimental data.

The main contribution into a linewidth of the plasma, under the above conditions, is made by the Doppler and collisional broadening. The linewidth makes 1.0?1.2 eV (without accounting of the Doppler broadening, connected with plasma motion), which corresponds to ? ? ?$1.5\cdot10^{15}$ 1/s for a resonant line of a He-like Al XII ion (??7.6 A). This allows one to estimate a cross-section of the radiation absorption in the maximum, $?_{max}=?e^2/mc\ 4/?\ ?$ ? $7\cdot10^{-18}$ cm$^2$. For the ion density $3\cdot10^{19}$ cm$^{-3}$ the width of a self-absorption zone is ?50 µm, which is comparable with the radiation bandwidth. So, one will observe a self-absorption effect for this line, which should lead to a line broadening and intensity decreasing at the line center. A due regard for this effect will improve an agreement between the experimental and calculated spectra of a collision-radiative model at a further stage of its development.

A detailed comparison of the experimental and theoretical spectra for an Al plasma (Fig.8a) illustrates a satisfactory agreement of the calculation and experimental data (a coincidence of relative intensities of the separate spectral lines). But as follows from Fig.8a, the widths of spectral lines obtained in an experiment are greater than those derived in calculations. This may be due to the fact that a Stark broadening of spectral lines, which is quite considerable for the transitions n=1> n?3 of H- and He-like ions, has not been taken into account sufficiently accurately. Beside, the satellites of resonance lines are not available either for the calculation spectra because auto-ionization states had not been considered in the ion level models. In addition, a recombination edge is absent in a short-wavelength spectral region, due to a recombination into an internal K-shell. The reason of this absence is

most likely due to the nonstationary effects. Due to characteristics temporal relationships, the free places in a K-shell are filled in a our calculations due to a collision excitation and deactivation, and not due to a recombination.

A comparison of Al plasma density profiles at different moments (see Fig.3) shows that they do not practically change with time. The electron temperature, on the contrary, changes essentially. For example, within the region of 0÷100 μm (which is the region of highest contribution into the radiation plasma energy), the electron temperature changes, at some points, by 10 and more times from 1÷2 keV to several tens eV, during 198 ps. A theoretical spectrum depicted in Fig.8a corresponds to the temperature of 500 eV. This is a circumstantial evidence of the plasma radiation both at an earlier and a later stages of the process, with account of the above time estimate of the plasma radiation.

For the copper plasma, the experimental and theoretical spectra differ considerably. The spectral calculations show that some of the intensive lines within 9.5÷12.5A are not available, as seen from Fig.8b. The fact is that initially, only the lines responsible for the 4-2 and 3-2 transitions in a Ne-like ion of CuXX were included into consideration. The calculations disregarded the dielectronic satellites of resonance lines because the auto-ionization states were not taken into account in the model of ion levels [6]. It is planned that the dielectronic satellites will be included into calculations at a following phase of the research. Moreover, in the calculations there were not considered some of the resonance lines of the ions CuXIX, CuXXI-CuXXV of the spectral region under study, due to the lack of the data on the oscillator forces and the probabilities of spontaneous radiative transitions. It is also seen that the wavelengths of several spectral lines do not coincide with the experiment while the intensity is very high. The reason of these discrepancies lies in the following. For some of the ions, one did not consider, in the schemes of levels, a splitting of electron configurations into therms corresponding to different values of the orbital momentum $L$ and a total spin $S$. Most vividly this is seen for the line with $l$=11.03A that corresponds to the transitions $2s^2 2p^4 3d$-$2s^2 2p^5\ {}^2P$ for the F-like ion of CuXXI. An upper state was considered with splitting into therms, in the scheme of levels. To the transition under study there corresponds an averaged value of the wavelength and a summary therm transition probability. An experimental spectrum of this line shows several corresponding spectral lines of less intensity with close wavelengths. An analogous situation has been observed for some other lines. A comparison of the experimental and calculation spectra showed clearly that a splitting of electron configurations into the therms is to be included in the schemes of levels of all ions. However, the main most intensive resonance lines that pertain to transitions between the levels of a Ne-like ion of CuXX showed an agreement between the theoretical spectra and the experimental data.

Density and temperature for the spectral calculations of copper were chosen so that relative intensities of the most intensive lines approximately coincided. The conditions that had been chosen ($T_e$=320 eV and $r$=0.1 g/cm$^3$) are in an agreement with the calculated profiles of density and temperature (Fig.4). The calculations showed that it is difficult to find such conditions under which the relative intensities

of most spectral lines coincided, because in experiment the time-integrated spectrum had been measured. As shown by the plasma evolution calculations (see section 3), the macroscopic parameters of the plasma ($N_e$, $N_i$, $T_e$) vary within a wide range during a pulse interaction with matter. We measured experimentally the radiation that is emitted from a relatively hot and rarefied plasma, at different instants, and from a relatively dense and cold plasma. This is confirmed by the results of spectral calculations plotted in Figs.7 and 8b. Figure 8b illustrates a considerable difference of 8÷9 A between the experimental and calculated spectra. An average degree of the ionization is 20.26. Under the given conditions, the spectral lines of CuXXVI-CuXXIX ions which are rather intensive on an experimental spectrum in this region, have a negligibly small intensity on a calculation spectrum and are not seen in the Figure. From Fig.7 it follows, however, that intensive spectral lines appear, in this region, at higher temperatures.

The results of calculations of a spectral emissivity of a copper plasma, within the framework of a Hartree-Fock model, were used in [8]. This quantum-statistical model of a self-consistent field proves to be a reliable and the only one means (despite the complex and lengthy calculations) for a calculation of spectral properties of high nuclear charge ions. In the model, the properties of an average ion (with average filling numbers) are considered, and a great number of states of ions and spectral lines are taken into account. A comparison of the experimental and theoretical spectra [8] is depicted in Fig.11. The calculations were made with a quantum energy step of $0.02 \cdot T_e$. Such a step does not allow one to perform a detailed comparison of separate spectral lines, but is quite sufficient for a qualitative analysis.

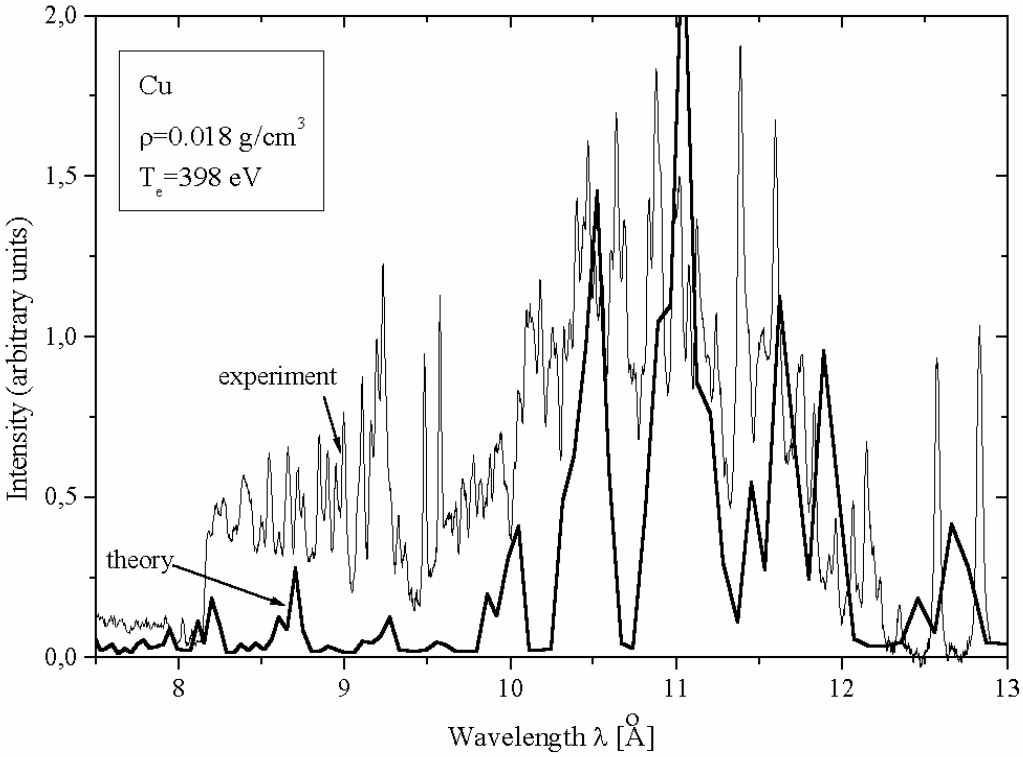


**Fig.11.** Comparison of the experimental spectrum with calculation results of Hartree-Fock-Slater model [8].

As seen from the comparison, the calculations made by a more sophisticated Hartree-Fock-Slater model allow one to repeat, sufficiently well, a spectral envelop. But as before, the stationary approach at the calculation of spectrums does not allow to reproduce all spectral particularity correctly.

In the case of an aluminum plasma, the spectrum was composed of the lines of only H- and He-like ions which are present simultaneously in the plasma in considerable quantities and at about the same temperatures. Therefore, a time-integrated experimental spectrum could be determined, with a good accuracy, by a single value of the temperature (the dependence of plasma properties on the density is less essential). The spectral lines responsible for a larger group of ions (CuXIX - CuXXIX) correspond to a copper plasma. But the main contribution into the radiation is made by the lines of a smaller group of the lines (CuXIX - CuXXII). The lines of CuXXIII - CuXXIX ions (unlike the calculation spectrum) have a considerable, though a lesser intensity. As seen from Fig.12, showing a dependence of relative concentrations of ion on temperature, the ions CuXIX - CuXXII are present in the plasma, in considerable mounts, at rather low temperatures, where the concentration of CuXXIII - CuXXIX ions are negligibly small, and otherwise. Because the experimental spectrum demonstrates a simultaneous existence of the lines of these two groups of ions, one might conclude that the plasma radiation processes are nonstationary. In particular, one should say that one group of the lines is irradiated at higher temperatures at an earlier stage of a process, and the other group, at a later stage and at lower temperatures.

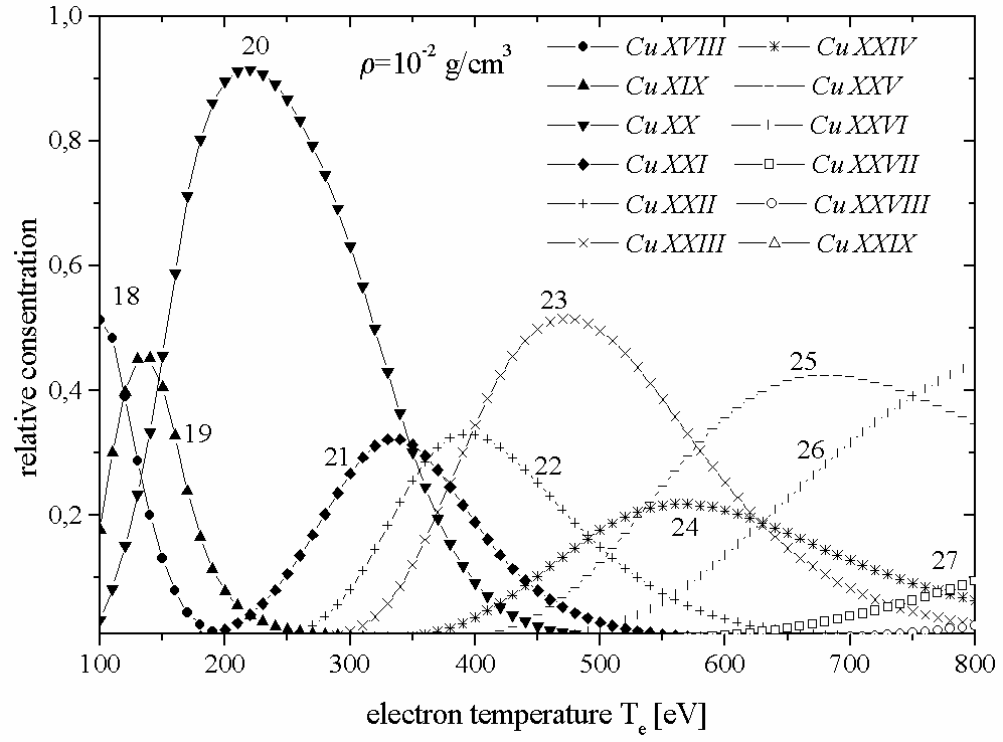


**Fig.12.** Relative concentration of multicharged ions in the plasma of copper as a function of electron temperature at density ?=$10^{-2}$ g/cm$^3$.

Thus, the observed relation between a dynamics of radiation of separate groups of lines with a spatial and temporal dynamics of a laser flare permits one to speculate about the nonstationary processes that proceed in the plasma even by analyzing the time-unresolved spectra. From a comparison of experimental and calculations results it follows that a linear radiation of a small group of ions constitutes the main part of radiative losses. A more accurate comparison of the calculations results with the time resolution measurement results would yield additional information about the processes occurring in the plasma.

Consider the calculation results of the spectrally integrated emissivity (Fig.10). An analytical character of dependences for the aluminum and copper plasmas is the same, and a further discussion will be valid for the plasmas of both elements. The estimates show that the maxima of the emissivity of a unit plasma volume, $P_{rad}$, coincide with the density maxima. This is due to the fact that $P_{rad} \sim N_i^2 \cdot \langle Z \rangle$. The plot $P_{rad}$ has two maxima, one of which is responsible for a solid-state body density region. But at such densities, the radiative paths are small, the plasma turns to be optically thick, and the radiation is found locked in a volume. So, the radiation might be recorded, experimentally, from a region of higher gradients of an electron temperature on the distance 50?60 μm from target. This region is also responsible for the maximum of the emissivity as calculated per ion, $W_{rad}$. The densities are rather small in this region and the plasma is optically transparent. It should be noted that the emissivity for aluminum and copper coincide, by an order of magnitude. However, as both $P_{rad}$ and $W_{rad}$ are proportional to the average degree of ionization, a characteristic scale of the radiative capability, for different elements, corresponds approximately to a charge of an element nucleus (13 for the aluminum and 29 for copper).

Thus, by comparing the calculation results with the results of measurements one can draw the following conclusions:

1. The radiative spectra correspond to an optically thin plasma; the data of calculations and experiments are an a satisfactory agreement.
2. The plasma irradiates during a long period (0.5 ns) which is many times longer than a laser pulse duration. In the case of copper, it may be possible that one group of the lines is irradiated at a higher temperature at an early stage of the process, and the other group, at a later stage at lower temperature and higher density of the plasma. The time resolution measurements may yield new information.
3. The basic parameters of the plasma (temperature, density, and other values) correspond to the calculation data, and one should take them into account at calculations of any atomic and/or nuclear processes.

This work is partially supported by ISTC (grant N856) and by physical educational - scientific center "Fundamental optics and spectroscopy" (in the context of Federal Target Program "Integration").

# References

1. V.S. Belyaev, V.I. Vinogradov, A.S. Kurilov, A.P. Matafonov, A.V. Pakulev, V.E. Yashin, *Kvantovaya Elektronika*,, **30**, p.229, 2000.
2. I.Yu. Skobelev, A.Ya. Faenov, B.A. Bryunetkin, S.A. Pikuz, T.A. Pikuz, V.M. Romanova, T.A. Shelkovenko, *ZHETP*, **56**, p.1234, 1995.
3. N.N. Demchenko, V.B. Rozanov, "Hydrodynamic model of a picosecond laser pulse interaction with condensed targets", *Preprint FIAN,* N 2, 2001.
4. G.A. Vergunova, V.B. Rozanov, “Influence of intrinsic X-ray emission on the processes in low-density laser targets”, *Laser and Particle Beams*, **17**, pp. 579-583, 1999.
5. G.A. Vergunova, E.M. Ivanov, V.B. Rozanov, "Collision-radiative calculation model of ionization content and levels populations of a nonequilibrium plasma (Al,Ar,Au)“, *Preprint FIAN*, N 12, 1998.
6. G.A. Vergunova, E.M. Ivanov, V.B. Rozanov, "Calculation of optical characteristics for nonequilibrium plasma of aluminum and copper", *Preprint FIAN*, N 74, 1999.
7. Ya.B. Zeldovich, Yu.P. Raizer, “Physics of shock waves and high-temperature hydrodynamic phenomena”, Moscow, “Nauka” Publ. House, 1966.
8. A.F. Nikiforov, V.G. Novikov, V.B. Uvarov, “Quantum-statistical models of high-temperature plasma an methods for a calculation of Rosseland mean paths and equations of state”, Moscow, FIZMATLIT, 2000.